The permeation properties of small organic cations in gramicidin A channels

Sang-Ah Seoh and David Busath
Section of Physiology, Brown University, Providence, Rhode Island 02912 USA

ABSTRACT The conductance properties of organic cations in single gramicidin A channels were studied using planar lipid bilayers. From measurements at 10 mM and at 27 mV the overall selectivity sequence was found to be $NH_4^+ > K^+ >$ hydrazinium > formamidinium > $Na^+ >$ methylammonium, which corresponds to Eisenman polyatomic cation sequence X′. Methylammonium and formamidinium exhibit self block, suggesting multiple occupancy and single filing. Formamidinium has an apparent dissociation constant (which is similar to those of alkali metal cations) for the first ion being 22 mM from the Eadie-Hofstee plot (G_0 vs. G_0/C), 12 mM from the rate constants of a three-step kinetic model. The rate-limiting step for formamidinium is translocation judging from supralinear *I-V* relations at low concentrations. 1 M formamidinium solutions yields exceptionally long single channel lifetimes, 20-fold longer than methylammonium, which yields lifetimes similar to those found with alkali metal cations. The average lifetime in formamidinium solution significantly decreases with increasing voltage up to 100 mV but is relatively voltage independent between 100 and 200 mV. At lower voltages ($\leq$100 mV), the temperature and concentration dependences of the average lifetime of formamidinium were steep. At very low salt concentrations (0.01 M, 100 mV), there was no significant difference in average lifetime from that formed with 0.01 M methylammonium or hydrazinium. We conclude that formamidinium very effectively stabilizes the dimeric channel while inside the channel and speculate that it does so by affecting tryptophan-reorientation or tryptophan–lipid interactions at binding sites.

INTRODUCTION

Gramicidin is an uncharged peptide that dimerizes head-to-head by six interchain N—H · · · O=C hydrogen bonds to form cation-selective channels with the internal diameter ~ 3.7 Å in lipid bilayer membranes (1, 2). It is a useful model of permeation for some membrane channels because it exhibits the properties of a cation-selective, single-filing pore (3, 4). The gramicidin channel permeability characteristics (single-channel conductance and single-channel lifetime) for the alkali metal cations have been investigated broadly (3, 5–7) and reviewed by Andersen (8), whereas those of polyatomic cations have not. Hille and colleagues (9–11) used a variety of polyatomic cations to obtain structural information about the "selectivity filter" of the Na, K, and AChR channels. Eisenman et al. (12) extended this approach to gramicidin, applying the Eisenman "selectivity sequence" concept. Reversal potential measurements with membranes containing many gramicidin channels (13) showed that the small organic cations—ammonium, hydrazinium, methylammonium, and formamidinium—readily permeate the gramicidin channels, whereas the larger organic cations—ethylammonium, dimethylammonium, guanidinium, aminoguanidinium, and hydroxyguanidinium—are negligibly permeant. They concluded the selectivity sequence of polyatomic cations in gramicidin A channel corresponds to the Eisenman sequence IX′. Recently, Busath et al. (2) demonstrated that guanidinium permeability is undetectable by using single channel measurements with asymmetrical solutions and a square voltage wave protocol. They concluded that guanidinium appears to permeate at least three orders of magnitude less frequently than formamidinium. Based on the rate of potassium current blocks (14), guanidinium and other small iminium cations, including acetamidinium and the protonated versions of urea, formamide, and acetamide, were shown to permeate about six orders of magnitude less frequently than formamidinium. Energy minimization computations were used to produce an adiabatic map of the energy profile for guanidinium, acetamidinium, and formamidinium entry (15). This method generally exaggerates the heights of barriers but nevertheless yielded high barriers (~9 kcal/mol) for the first two cations and a low barrier (~4 kcal/mol) for the third ion, qualitatively consistent with the measured permeabilities.

The main factors that affect single-channel lifetime are surface tension of the membrane (16, 17), the membrane thickness (16–20), the membrane potential (3, 21), the salt concentration (3, 18, 21, 22) and the surrounding temperature (23, 24). Tl^+ and Ag^+ produce relatively long lifetimes compared with those of alkali metal cations in the gramicidin A channel (25, 26). More recently, Becker et al. (27) found that Trp^{11} near the metal cation binding site plays an important role in determining single-channel lifetime and concluded that indole groups of tryptophans alter channel duration through direct interactions with adjacent lipid and H_2O. In this article we fully examine the single-channel conductance vs. concentration and voltage and single-channel lifetime characteristics of methylammonium and formamidinium and, to a more limited extent, hydrazinium. We report that the low concentration transport selectivity sequence (which reflects the barrier heights for the first ion occupancy) (28, 29) of the polyatomic cat-

Address correspondence to Dr. David Busath, Box G-B3, Brown University, Providence, RI 02912.

ions in the gramicidin A channel follows Eisenman sequence X′ rather than IX′; that based on the Eadie Hofstee plot, formamidinium has an apparent binding affinity that is similar to those of the alkali metal cations, though lower than Tl^+ or Ag^+; and that single formamidinium ion binding induces long single-channel lifetimes.

METHODS

In the general method, lipid bilayers were formed on the aperture of a polyethylene pipette inserted into the rear of a Teflon chamber as described previously (30). The lipid solution was a dispersion of glyceryl-1-monoolein (50 mg/ml) in *n*-decane or hexadecane and was painted on the pipette aperture and allowed to thin spontaneously to form bilayers. All the solutions were prepared freshly using distilled water purified to >18.2 MΩ-cm with a Barnstead NANO pure II system (VWR Scientific, San Francisco, CA) and were filtered just before use with a 0.2 μm Nalge Filter (Fisher Scientific, Pittsburgh, PA). Formamidine · HCl, methylamine · HCl, and hydrazine · HCl were used without purification. To avoid contamination by NH_4^+ (which is very permeant in the gramicidin A channel), we tried to recrystallize the organic cations from several solvents, but the best purity was obtained, judging by the stability and magnitude of the current by simply using freshly prepared solutions. Salts were stored in a desiccator, and the single channel currents were measured within 1.5 h of solution preparation. This was particularly important for formamidinium, which underwent hydrolysis at a rate of ~5%/d according to the rate of appearance of formamide measured with ^{1}H-nuclear magnetic resonance (NMR). The magnitude of the formamidinium single channel current was increased due to contamination by 3–10% (in 1 M solution, more so at lower concentration) in 1 h, whereas in the case of methylammonium such changes were not observed. The transmembrane current was measured in symmetrical solutions, low-pass filtered with an RC filter using a cutoff frequency of 30 or 3,000 Hz and digitized with 12-bit resolution at 100 or 10,000 samples/s for subsequent analysis with a Masscomp (Concurrent Computer Corp., Oceanport, NJ) computer. Single-channel currents using gramicidin A purified in our lab were similar to those reported by other labs (3, 31). All the single-channel currents were collected within 10–15 min after a lipid membrane was made. For each statistic, the number of channels utilized (n) is given in parentheses. The electrode asymmetry potential was checked before and after every experiment and was always <1 mV. The electrode potential drift was more significant in high salt solutions, i.e., more than 3 M chloride salt. The electrode potential was offset just before making each membrane and after data collection. All data collected during experiments where the shift of the electrode potential was >1 mV were discarded. All the measurements were performed at room temperature (20–26°C), and conductances were corrected to 25°C using Q_{20} = 1.9 (3).

For the measurement of the single-channel current with 10 or 27 mV in the concentration range of 0.01–2 M, 9 mM $MgCl_2$ was added to the solution. This is important to maintain a sufficiently low solution resistance to screen surface-charge contaminants and to minimize interfacial-polarization effects for the lowest concentrations of permeant ions (7, 32–34). The single-channel lifetimes for all the ions except formamidinium are relatively short, so for low concentrations and voltages the experiments were done in GMO (glyceryl-monoolein)/hexadecane membranes and confirmed in GMO/decane membrane for formamidinium. In addition, the cutoff frequency was reduced to 5–20 Hz and the sampling frequency to 15–60/s.

Current–voltage-concentration curves were fit using the unmodified symmetric seven-parameter, three-barrier, two-site (3B2S) model (35) with all rate constants dependent exponentially on voltage. Initial values for association and dissociation rate constant parameters were derived from Eadie–Hofstee plots (5, 36). This model has weakness, including, for instance, that the rate constant for the long translocation step is given an exponential voltage dependence, although it is more reasonably considered as electrodiffusion (37, 38). However, it was used for ease of comparison to previous experimental results and simplicity and is known to give predictions similar to electrodiffusion (37). The curve-fitting algorithm was the same as used previously (39). To find the best fit to all of the data simultaneously, we found it necessary to constrain most of the parameters, varying small groups (2–3) parameters at a time before a global minimization was attempted. For the global minimization, the increase of the second ion exit rate was fixed but the remaining six parameters were free.

Single channel lifetimes were measured by matching channel appearance steps with disappearance steps. When ambiguities existed due to simultaneous appearance of multiple channels with equal conductances, the match was randomized. This approach is less sophisticated than a probabilistic assignment and could bias the lifetime distribution, but it produces the correct average lifetime, which is the parameter of interest here and, in any case, is only rarely utilized because channel densities were purposely kept low.

RESULTS

Fig. 1 shows the single-channel currents and corresponding current histograms for three small organic cations: methylammonium, formamidinium, and hydrazinium in normal gramicidin A channels (1 M, 100 mV). The mean single-channel currents were 3.09 pA (n = 2,488), 1.55 pA (n = 777), and 2.97 pA (n = 109), respectively. The single-channel lifetimes were 0.55 s (n = 359), 2.41 s (n = 301), and 0.68 s (n = 101), respectively, in GMO/decane membranes. The single-channel lifetimes with formamidinium is around four to five times longer than those with the other two ions. Also evident, although we make no attempt to quantify it, is the open channel noise with formamidinium that is significantly greater than the baseline noise. This is not the case for methylammonium and hydrazinium. Fig. 2 demonstrates the voltage dependence of the open channel noise in the formamidinium solution. Increasing the membrane voltage seems to decrease the open channel noise. This behavior is similar to the voltage dependence of the open channel noise in Ag^+ solution (26). The fluctuations would seem to be due either to temporary channel closures or fluctuations in the current through an open channel. In the first case, the noise should increase with membrane potential because the dimer is destabilized with increased membrane potential in formamidinium solution. We observe that the noise decreases with voltage, which therefore favors the second possibility.

Figure 3 *a* shows the double logarithmic plot of conductance at 100 mV versus concentration of methylammonium and formamidinium. Both show saturation, with maxima at 3 M, and decreased conductances at higher concentrations. These downturns, possibly caused by the high cation reentry rate producing self-block, suggest that organic cations, like alkali metal cations, can multiply (at least doubly) occupy the gramicidin A channel. It is noteworthy that formamidinium

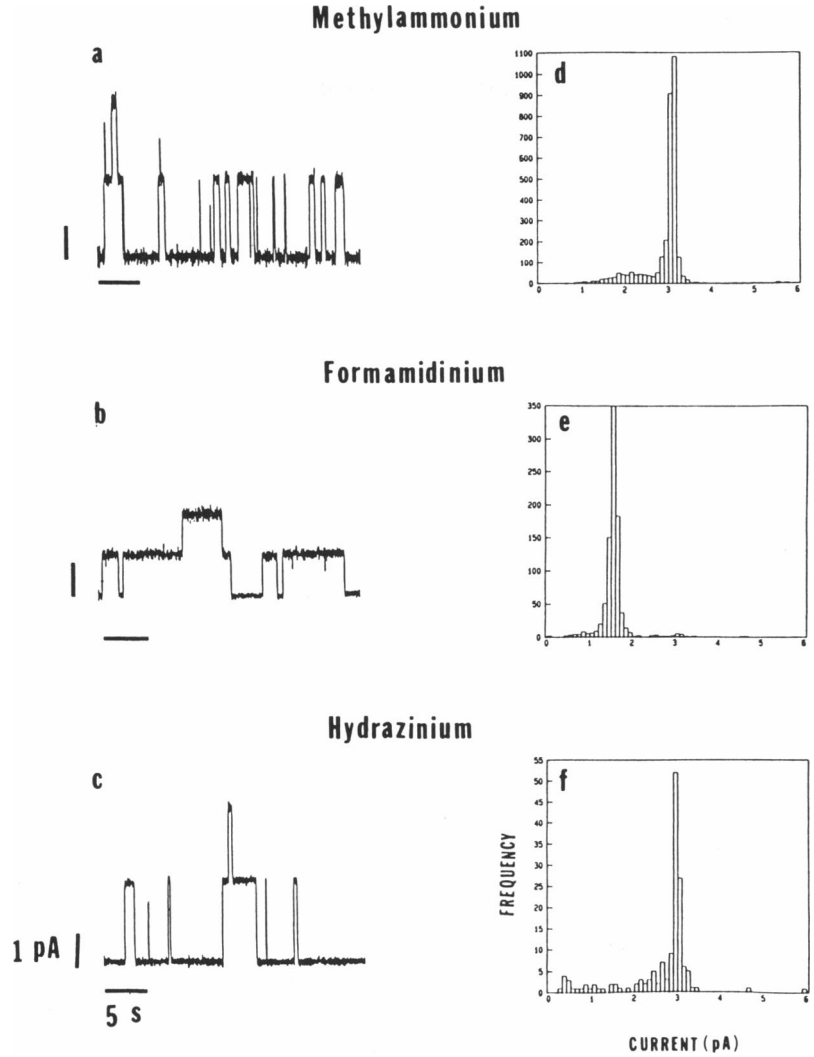

FIGURE 1 Single channel currents (*a–c*) and corresponding current histograms (*d–f*) with 1 M salt solutions at 100 mV in GMO/decane membrane. (*a* and *d*) Methylammonium; (*b* and *e*) formamidinium; (*c* and *f*) hydrazinium. All the data were collected within 1.5 h of solution preparation at room temperature (23–23.5°C), and histograms were corrected to 25°C using Q_{20} = 1.9.

conductance exceeds methylammonium conductance at low concentrations, where ion entry would be rate limiting.

Fig. 3 *b* shows the Eadie-Hofstee plots for the conductance (G_0) versus conductance/concentration (G_0/C). G_0 was approximated as the average conductance at ±10 mV. The low applied voltage was crucial, especially for formamidinium, since the experimental current–voltage (*I-V*) relations were supralinear at all the concentrations (0.1, 0.5, and 1 M) (Fig. 4), even between the applied voltage 10 and 25 mV (data not shown). Thus even at ±25 mV the apparent or experimental dissociation constants (K_1 and K_2) would be overestimated and the binding affinities underestimated for the first ion and second ion on the Eadie-Hofstee plots. In the low concentration range, an Eadie-Hofstee plot experimentally provides an estimate of the dissociation constant of the first ion, K_1, and in the high concentration range an estimate of the dissociation constant of the second ion, K_2 (4, 40, 41). In Fig. 3 *b* the K_1's ($B/2A$, defined in legend of Fig. 3 *b*) are 114 mM for methylammonium and 22 mM for formamidinium. The binding affinity (the logarithm of the reciprocal of the dissociation constant) (42) of the first formamidinium was around 1.8 times higher than that of methylammonium.

Figure 4 shows the *I-V* relationship for (*a*) methylammonium and (*b*) formamidinium. For methylammonium, the *I-V* relations are linear at 1 M, a little bit sublinear at 0.5 M, and sublinear at 0.1 M, which probably reflects a shift of the rate-limiting step from the voltage-independent entry via aqueous diffusion at low concentrations to the more voltage-dependent translocation at high concentration (43). The shapes of the *I-V* relations for formamidinium from experimental data were supralinear at all concentrations (0.1, 0.5, and 1 M) even at

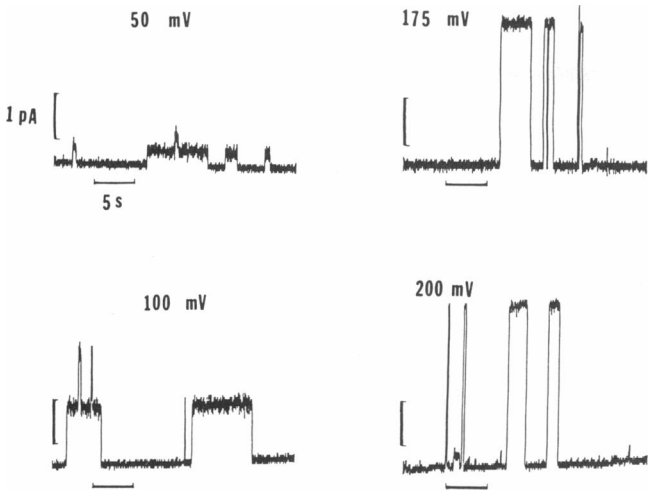

FIGURE 2 The voltage dependences of the open channel noise from 0.5 M formamidinium solution in gramicidin A channel in GMO/decane membrane. The sampling frequency was 100/s, and the cutoff frequency was 30 Hz.

0.01 M (see Table 2), which indicates that the main energy barrier for formamidinium is translocation through the channel (44).

Table 1 shows rate constants predicted by 3B2S model and used in the theoretical curves in Figure 3. Formamidinium has a relatively stronger binding affinity than methylammonium, high apparent repulsion between ions, and lower translocation rate than exit rate. Methylammonium has a higher translocation rate than exit rate.

Figure 5 shows the double reciprocal plot of 1/current versus 1/concentration at 10 and 100 mV for both experimental data and theoretical predictions from the 3B2S model. With these axes, the rectangular hyperbola relationship expected for a single-ion pore yields a straight line with an x-intercept at $-1/K_1$ ($= -2A/B$). Deviations from a straight line can be explained most easily as multiple-occupancy effects. Except for methylammonium at 100 mV, curvature can be detected in each case and is especially marked for formamidinium at 10 mV, from which we conclude that both ions produce multiple occupancy. The intercept for the 10 mV methylammonium would be near $-9\ M^{-1}$ if an extrapolation based on the rightmost two points was done, consistent with the first-ion apparent dissociation constant of 114 mM obtained from the Eadie-Hofstee plot. The theoretical curves from the 3B2S model show a qualitatively reasonable fit at both voltages.

For formamidinium, the 10-mV data extrapolates to $-1/K_1 = -45\ M^{-1}$, where K_1 is consistent with the apparent first-ion dissociation constant of 22 mM, obtained from the Eadie-Hofstee plot. The rightmost 100-mV data points extrapolate to $-18\ M^{-1}$, suggesting that the apparent first ion affinity is lower at the higher membrane potential. The theoretical curves fall below the data at both voltages. This format most exaggerates the weakness of the 3B2S fit that were also apparent in the

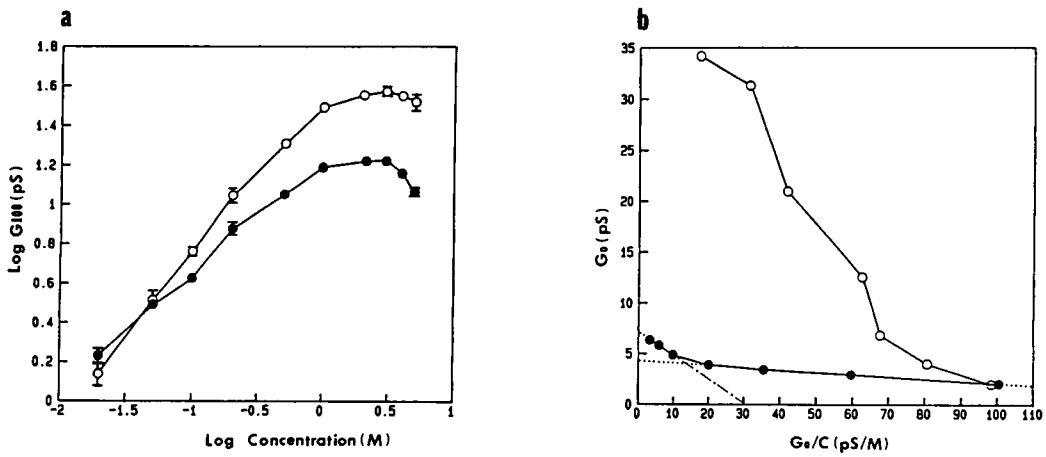

FIGURE 3 (*a*) Double logarithmic plot of single-channel conductance in the salt concentration range 0.02–5 M and at the applied voltage 100 mV. (○) Methylammonium; (●) formamidinium. Each point is from the averaged standard channel peak (n = 500–4,000), and all the data were collected within 1.5 h of solution preparation. GMO/decane membrane. 25°C. Vertical bars represent standard errors that were obtained from ≥7 up to 41 experiments. In all the data points that do not have bars, standard errors were within the sizes of the symbols. The range of all the standard errors was from ±0.01 to ±0.06 in log units. (*b*) Eadie–Hofstee plot, G_0 vs. G_0/C, at the applied voltage ±10 mV. All the salt solutions (0.02–2 M) were augmented by 9 mM $MgCl_2$. The collecting cutoff frequency was 10–20 Hz, the sampling frequency was 30–60 Hz. (○) Methylammonium; (●) formamidinium. The slope at low formamidinium concentration (designated line with · · · ·) equals $-K_1$ ($-B/2A$ in the two site model of reference 5) and the slope at high concentration (designated line with · – · – ·) equals $-K_2$ {$-2KE/D(K+E)$, see reference 5}, where A is defined as the rate constant of entry to empty pores from left and right. (*B*) Exit from singly occupied pores; (*D*) the rate constant of entry to singly occupied pores from left and right; (*E*) exit from doubly occupied pores; and (*K*) transfer between the ends of the pore. All the data were collected within 1.5 h of solution preparation. GMO/decane membrane. 25°C. Standard errors of means were within sizes of symbols and their ranges were ±0.036 to ±0.17 pS in the formamidinium solution and ±0.0024 to ±0.41 pS in the methylammonium solution. Data points are connected by lines to facilitate grouping.

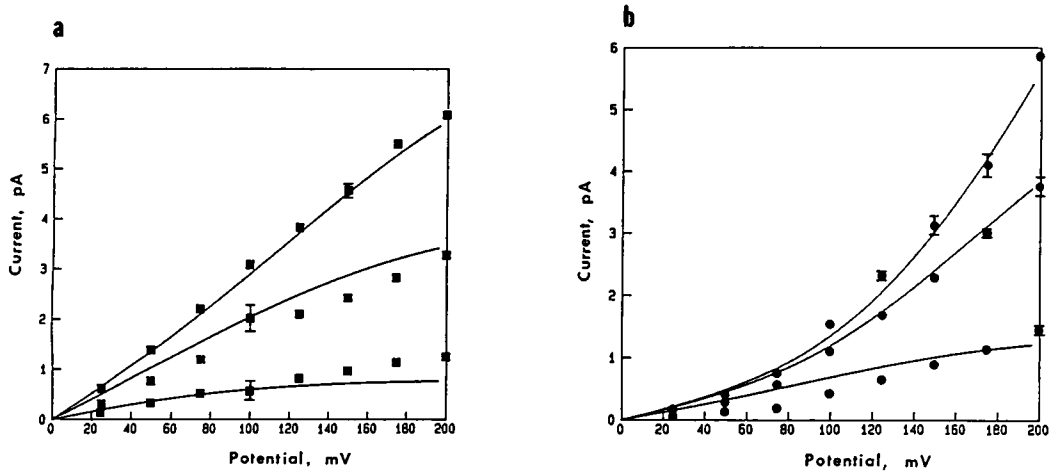

FIGURE 4 The *I-V* relationship for methylammonium (*a*) and formamidinium (*b*). The applied voltage step of 25 mV tilted to 200 mV in 1, 0.5, and 0.1 M symmetrical solutions in GMO/decane membranes at 25°C. All the data points were averaged standard single-channel currents of 200–600 channels collected within 1.5 h of solution preparation. The solid lines represent the predicted *I-V* curves from the three-step, two-site model. Vertical bars represent standard errors that were obtained from ≥4 up to 16 experiments. In all the data points that do not have bars, standard errors were within the sizes of the symbols.

formamidinium *I-V*s (Figure 4 *b*). We suppose that the problems are due to the simplification of a one-step translocation process. Nevertheless, the 3B2S model does provide an approximate estimate of the apparent dissociation constant for first ion, within a factor of two for both methylammonium and formamidinium. The data are better fit in methylammonium solution (*a*) than formamidinium solution (*b*).

Table 2 shows the single-channel conductance measurements using 10 mM permeant cation (augmented by 9 mM $MgCl_2$) at 27 and 100 mV. For alkali metal cations, the conductance measurements at 10 mM and at 27 mV give the same conductance ratio as the permeability ratio, which means that the principle of independence apparently applies for the gramicidin A channel at low concentration and low applied voltage (45). In our data G_{Na}/G_K is 0.338 at 27 mV and 0.381 at 100 mV in GMO/hexadecane membrane. These ratios are consistent with the results of Decker and Levitt (45) (0.34 at 27 mV and 0.41 at 100 mV in GMO/hexadecane membranes) and with the permeability ratio (P_{Na}/P_K = 0.27 in GMO/hexadecane membranes) estimated from the reversal potential measurement in 10-mM biionic conditions (46). The results of Table 2 for organic cations similarly can be compared with previous reversal-potential data (13) based on permeability ratios because the dissociation constant (B/A) for the first formamidinium ion is ~44 mM (Figure 3 *a*). Table 2 shows that formamidinium is less permeant than K^+ in the gramicidin A channel ($G_{formamidinium}/G_K$, G_f/G_K = 0.5 in both GMO/decane and GMO/hexadecane membranes at the applied voltage, 27 mV), which is contradictory to the estimate based on the reversal potential, $P_{formamidinium}/P_K$ = 1.55. $G_{methylammonium}/G_K$ is 0.26, consistent with $P_{methylammonium}/P_K$ = 0.24, and $G_{hydrazinium}/G_K$ = 0.7 is similar to $P_{hydrazinium}/P_K$ = 0.9. The explanation for the inconsistency in the formamidinium results probably lies in the fact that the solution used by Eisenman et al. (13) was significantly contaminated by NH_4^+, which is more permeant than K^+. Judging from the appearance of formamide in the solution (detected by ^{1}H-NMR), we estimate that our fresh solution contains <3% NH_4^+. We find that the permeability sequence in gramicidin A channel is K^+ > hydrazinium > formamidinium > Na^+ > methylammonium.

Figure 6 *a* shows histograms of the single-channel lifetimes in 1 M formamidinium (mean = 11.36 s, 21.5°C) and methylammonium (mean = 0.60 s, 22°C) solutions with GMO/decane membranes. Figure 6 *b* shows the change of single-channel lifetimes in formamidinium solutions (0.1 and 1 M) and methylammonium solutions (1 M) with increasing applied membrane potential. The single-channel lifetime in 1 M formamidinium solution is higher than that in 0.1 M formamidinium solution. In the case of 1 M methylammonium, the single-channel lifetime increased with the increasing voltage. In the case of formamidinium, the mean channel lifetime is much longer than that for methylammonium even at 0.1 M: 0.40 s for methylammonium at 23°C (data not shown) versus 4.22 s for formamidinium at 25 mV (Figure 6 *b*). It decreases significantly with the increasing membrane potential in 0.1 and 1 M formamidinium concentrations, whereas it increases in 1 M (Figure 6 *b*) or 0.1 M (data not shown) methylammonium solution.

These decreases of single-channel lifetime with increasing voltage were most dramatic at low applied potentials. Likewise, the average channel lifetime increased at low temperatures, particularly at low voltages as is shown in Figure 7. Together, Figures 6 and 7 suggest that formamidinium dramatically stabilizes the channel,

TABLE 1 **Rate constants predicted by the curve fitting**

Constant	Formamidinium (χ^2 = 3.95)	Methylammonium (χ^2 = 3.15)
$A_{01,02}$ (10^7 M^{-1} s^{-1})	22.4	4.86
$B_{10,20}$ (10^6 s^{-1})	5.45	5.74
$D_{13,23}$ (10^7 M^{-1} s^{-1})	14.0	5.63
$E_{31,32}$ (10^8 s^{-1})	385.0	2.31
$K_{12,21}$ (10^6 s^{-1})	2.84	14.60
B/A (mM)	24	118
B/K	1.9	0.4
δ_1	0	0
δ_2	0	0.19

The resulting rate constants for methylammonium were interpreted to represent the following energy profile parameters: a small entry barrier (+1.415 RT) and deep well depth (−10.184 RT) for the first ion, a large the translocation barrier (+0.481 RT), a slight change of the entry barrier (−0.147 RT) upon second ion occupancy, and a change of the well depth (+3.55 RT) upon second ion occupancy (perhaps due to the electrostatic repulsion between the two ions). The positions of the entry barrier and well were 0 and 19% through the applied electric field, respectively.

The rate constants for formamidinium yielded the following: entry barrier (−0.112 RT) and well depth (−11.763 RT) for the first ion, and translocation barrier (0.54 RT) for the first ion, changes of entry barrier height (+0.466 RT) and of well depth (+9.33 RT) upon double occupancy, and entry barrier and well positions both 0% through the applied electric field. These values are based on the usual Eyring rate theory equations (reference 29) with the following modifications: (*a*) a low transmission coefficient (0.1) was used for the translocation step to simulate the high probability of reentrant trajectories and (*b*) the preexponential constant for the entry step was taken as the collision rate, 10^9 M^{-1} s^{-1} (similar to values suggested for alkali metal cations in reference 4). The exit step was assumed to be a single short activated step, so the Eyring transmission coefficient was set to 1.

$A_{01,02}$, access to empty pores from left (01) and right (02); $B_{10,20}$, exit from singly occupied pores; $D_{13,23}$, access to singly occupied pores from left (13) and right (23); $E_{31,32}$, exit from doubly occupied pores; $K_{12,21}$, transfer between the ends of the pore; δ_1, voltage dependence parameter for entry; δ_2, voltage dependence parameter for exit. The voltage dependence parameter for translocation is $0.5 - \delta_1 - \delta_2$. B/A is the calculated dissociation constant for the first ion and B/K is the ratio of the exit rate to the translocation rate for the first ion. The reduced χ^2 was calculated using the equation in reference 39 with standard deviations of ±0.04 for formamidinium and ±0.08 for the methylammonium.

probably from a site in the channel whose occupancy is very voltage, concentration, and temperature dependent. Table 3 shows that the addition of 1 M KCl to the formamidinium solution significantly reduces the stabilizing effect of formamidinium, indicating that stabilization is due to binding at a specific site.

Table 4 shows the effect of concentration on single-channel lifetimes of formamidinium and methylammonium. In both cases channel lifetimes increase with the increasing concentration (in the range of 0.05–1 M) and slightly decrease at 2 M. The total single ion occupancy by formamidinium predicted by the kinetic model is relatively constant and high in the concentration range of 0.1–1 M (0.891–0.986), and the double occupancy is very low even at 1 M (0.0014) because of the strong binding affinity and high second ion leaving rate. From this, we can only suppose that either slight changes in occupancy must have large effects on channel lifetime or that the same shift in transport kinetics that raises conductance (Figure 3 *a*) with increasing concentration is somehow responsible for stabilization. In any event, we suppose that binding of formamidinium in the channel mediates the stabilization. If formamidinium binding stabilizes the gramicidin dimer more effectively than binding of other cations, then, in the limit of low occupancy and at the relatively high voltage (≥100 mV), the channel lifetime should be independent of ion species. This is found to be the case, as shown in Figure 8. The mean single channel lifetime in 0.01 M formamidinium solution at 100 mV, 1.94 s was not different from those of others in the same experimental condition: methylammonium (mean = 1.42 s) and hydrazinium (mean = 1.88 s) in GMO/hexadecane bilayers (used to enhance channel lifetime for these low conductance measurements).

DISCUSSION

Permeability

From the bend in the double reciprocal plots, it appears that the gramicidin channel exhibits more than one binding affinity for methylammonium and formamidinium. If the channel has two equivalent binding sites, one in each monomer as has been demonstrated for the alkali metal cations (47, 48), this indicates that the affinity must change with occupancy. Alternatively, the organic ion might bind at additional sites of differing affinities in the channel, such as the monomer–monomer junction. The self-block in the concentration–conductance curve suggests a saturated multiple-occupancy, single-filing pore (49–51). Formamidinium has a relatively strong binding affinity as evidenced by the saturation at low concentration and the position of the foot in the Eadie-Hofstee plot, which suggests that for binding of the first ion, B/A = 44 mM. This is similar to those of the alkali metal cations (52), but much weaker than that of Tl^+ (K_1 = 1 mM) (53, 54). Methylammonium binding (B/A = 228 mM) is much weaker than alkali metal cation binding.

The current–voltage (I-V) relation for formamidinium is supralinear (Figure 3 *b*), even at concentrations as low as 0.01 M (Table 2), even though the conductance is comparable with the Na^+ conductance. This is unusual: the I-Vs for all other ions studied to date are sublinear at these concentrations. In the past, the shift to supralinear I-Vs at concentrations in excess of 1.0 M for the alkali metal cations has been taken to indicate that the rate-limiting step shifts from diffusion-limited entrance to voltage-dependent translocation at high concentrations (43). By this logic, formamidinium is translocation limited even at fairly low concentrations, suggesting that the mobility in the channel is lower than that of the alkali metal cations. However, the high formamidinium permeance indicates that formamidinium diffu-

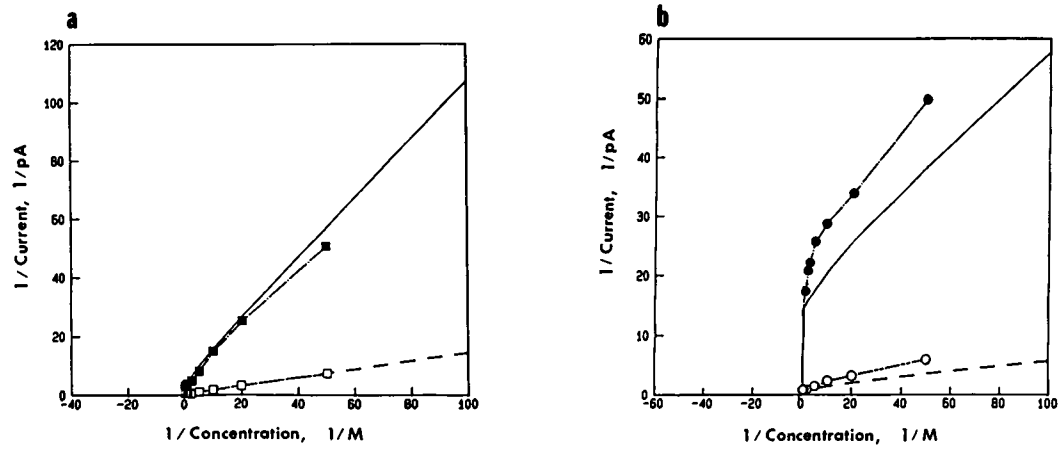

FIGURE 5 Double reciprocal plot for experimental data at 10 mV (*filled symbols*) and 100 mV (*open symbols*) and predictions from curve fittings (solid lines at 10 mV, dashed lines at 100 mV). (*a*) Methylammonium (■, data at 10 mV; □, data at 100 mV). (*b*) Formamidinium (●, data at 10 mV; ○, data at 100 mV). The dotted lines are extrapolations to $-1/K_i$ from the experimental data and the predicted curve. All the standard errors were within the sizes of the symbols and ranged from ±0.02 to ±1.3/pA for methylammonium and ±0.16 to ±0.89/pA for formamidinium.

sion up to and entry into the channel are comparable with those of alkali metals. This dilemma is further evidenced by the 3B2S shown in Figure 3 *b*. The model could not produce the high conductance at 1 M and also the supralinearity at 0.1 M simultaneously given the diffusion limited entry rate that was not allowed to exceed 10^9/mol·s. Therefore, supralinearity in the 0.1-M curve was sacrificed. These arguments lead us to speculate that supralinearity may be partially due to voltage-dependent peptide conformational changes.

The high formamidinium affinity is probably due to multiple hydrogen bonds between the four charged donor hydrogens of the cation and the channel backbone carbonyls. The formamidinium motility in the channel could be low due either to hydrogen bonds or steric interactions with the walls of the channels. An adiabatic map of the interaction energies along the transport reaction coordinate (15) computed with an empirical force field indicates that the steric hindrance (more precisely, unfavorable van der Waals contact) is negligible for formamidinium and that the ion forms two to four hydrogen bonds with the backbone at all points along the pathway. Hydrogen bonds formed by formamidinium should be stronger than those formed by amines due to stabilization of the resonating double bond and ionic charge. These would produce high affinity and may also cause low ion motility in the channel which may also contribute to supralinearity.

Methylammonium is smaller than formamidinium, has few hydrogen bond donors (three rather than four), and has an aliphatic methyl group. The hydrophobic methyl group would be expected to partition out of bulk water to reduce its ordering effect on waters in the solvent shell. However, the reduced number of hydrogen bonds and the steric constraints imposed by the methyl that prevent the ion from rotating readily in the channel appear to give methylammonium a lower binding affin-

TABLE 2 Low concentration conductance

Ions	27 mV		100 mV	
	G_i	G_i/G_K	G_i	G_i/G_K
	pS		*pS*	
GMO/*n*-hexadecane membrane (31 Å)				
K^+	2.96 ± 0.27	1	2.18 ± 0.07	1
Na^+	1.00 ± 0.07	0.338	0.83 ± 0.02	0.381
Methylammonium	0.78 ± 0.04	0.260	0.73 ± 0.04	0.335
Formamidinium	1.48 ± 0.07	0.500	1.58 ± 0.06	0.723
Hydrazinium	2.13 ± 0.06	0.720	1.72 ± 0.06	0.789
GMO/*n*-decane membrane (47 Å)				
K^+	2.74 ± 0.002	1	2.16 ± 0.127	1
Formamidinium	1.37 ± 0.033	0.50	1.46 ± 0.141	0.68

Conductance (mean ± SD) ratio at low salt concentration, 10 mM with 9 mM $MgCl_2$ added to shield contaminant surface charge. All the data for the three small organic cations were collected within 1.5 h and, for K^+ and Na^+, within 3 h of solution preparation.

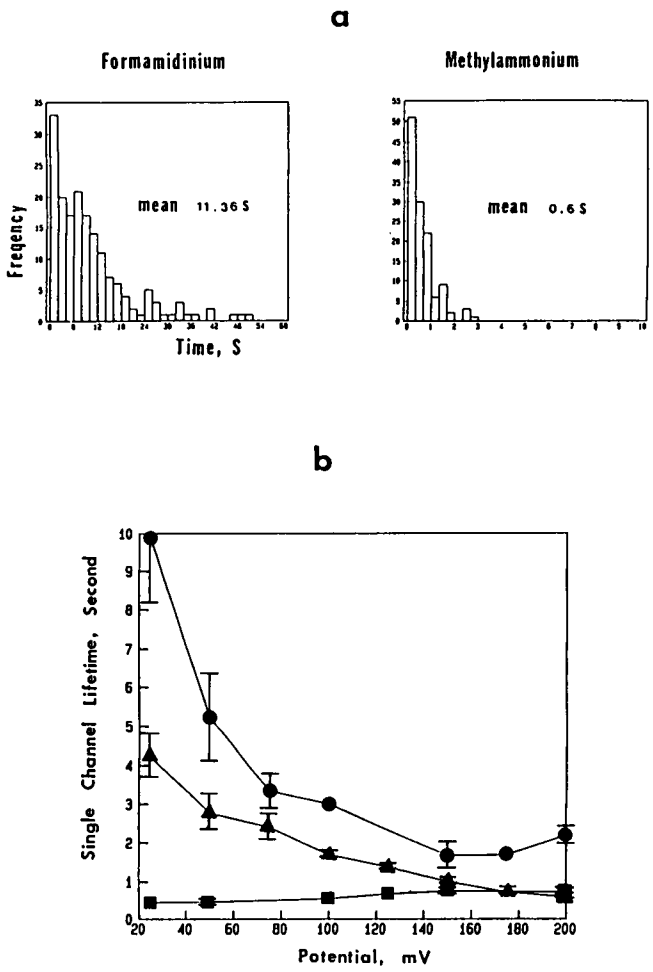

FIGURE 6 (*a*) Single-channel lifetime histograms in formamidinium (*left*) and methylammonium (*right*) (GMO/decane membrane, 25 mV, 1 M salt + 9 mM $MgCl_2$). The mean single-channel lifetime in formamidinium was 11.36 s (21.5°C) and that in methylammonium (22°C) was 0.60 s. (*b*) The mean single-channel lifetime for formamidinium and methylammonium solutions in GMO/decane membranes as functions of membrane potential. (●) 1 M formamidinium solution at 24.5–25.5°C ($200 < n < 2{,}250$); (▲) 0.1 M formamidinium solution at 22–23°C ($330 < n < 1{,}900$); (■) 1 M methylammonium solution at 23°C ($270 < n < 450$). The n in parentheses is the number of channel lifetimes averaged for each data point. Vertical bars represent standard errors that were obtained from at least three experiments.

ity than formamidinium. Compared with ammonium, methylammonium again has fewer hydrogen bond donors, would be rotationally less mobile, and should also therefore have a lower affinity. Indeed, we found it to have a lower affinity than alkali metal cations, which in turn were found by Urban et al. (4) to have a lower affinity than ammonium.

Prediction of rate constants for formamidinium and methylammonium in gramicidin A channels using 3B2S model

The two-site model can be used to account for the current–voltage-concentration data semiquantitatively.

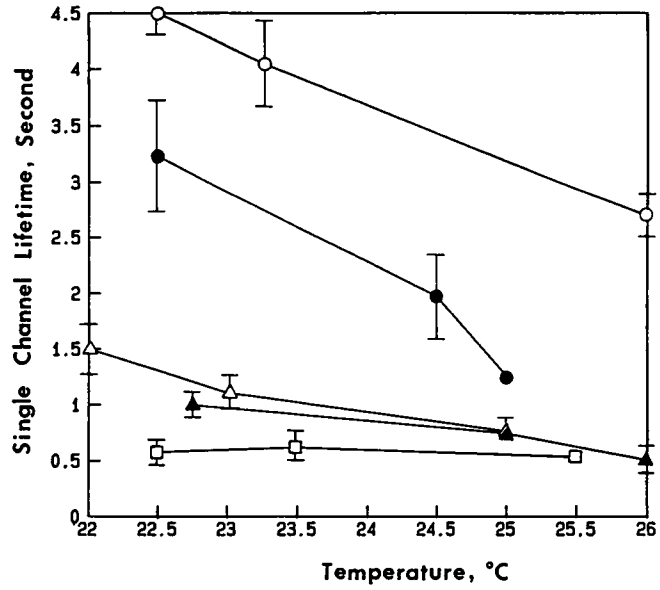

FIGURE 7 Temperature effect on the single-channel lifetime (s) in 0.1 M formamidinium solution with the increasing voltage (○, 25 mV; ●, 50 mV; △, 125 mV; ▲, 150 mV; and □, 200 mV) in GMO/decane membranes. Each data point represents an average of n channels ($150 < n < 1{,}914$). Vertical bars represent standard errors that were obtained from ≥5 up to 24 experiments. In all the data points that do not have bars, standard errors were within sizes of symbols.

The fits shown in Figures 3 and 4 have some weaknesses, however, as was noted above. These are partly due to inconsistencies in the data. In particular, the points at 100 mV are higher than expected in a few cases, probably because these represent the mean of results from a large number of experiments, some of which may have suffered from slight ammonium contamination. The model predictions for methylammonium have too high a conductance at 0.5 M and are too sublinear at 0.1 M. For formamidinium, the low voltage conductances are too high at all three concentrations and the 0.1 M predictions are sublinear, whereas the data are supralinear. The overestimate of conductance at low voltages for formamidinium is also apparent in the double reciprocal plot (Figure 4 *b*). Although it is well established that the long translocation step is best considered a diffusive process (37), we have utilized the 3B2S model for simplicity. It has been shown that the rate theory and Nernst–Planck

TABLE 3 The comparison of single channel lifetimes between pure and mixed salt solutions

Solutions	Lifetimes*
	s
0.1 M formamidinium (23°C)	4.20 ± 0.64
1 M K^+ + 0.1 M formamidinium (23°C)	1.15 ± 0.52
1 M K^+ (22°C)	0.67 ± 0.23

* Means ± SD.

TABLE 4 **The comparison of single-channel lifetime and probabilities of ion occupancies predicted by 3B2S model with the increasing salt concentration at 100 mV in GMO/decane membrane (20.5–21.5°C)**

Concentration	Formamidinium	Methylammonium
M		
3	— (0.992, 0.0042)	— (0.767, 0.218)
2	5.87	0.66 (0.818, 0.155)
1	5.99 (0.986, 0.0014)	0.74 (0.853, 0.081)
0.5	2.46 (0.976, 0.0007)	0.60 (0.818, 0.039)
0.2	1.56	0.43 (0.663, 0.013)
0.1	— (0.891, 0.00013)	0.41 (0.492, 0.005)
0.05	1.19	

The averaged channel numbers for single-channel lifetimes were 101–1,124. The two numbers in parentheses reflect the total single ion occupancy, $P_{01} + P_{10}$, and double occupancy, respectively.
There may be a competition between the stabilizing effect and a destabilizing effect due to ion–ion repulsion when the probability of the double occupancy increases (i.e., at 2 M).

approaches yield similar predictions, both for single ion (37) and multiion (55) channels. Likewise, alkali metal conductance data that can be reasonably well fitted with a 3B2S model (4) is also well fitted with Brownian dynamics (38). Generally, the voltage dependence of the conductance differs between discrete rate theoretical and continuum diffusion models, but the effective rate constants are similar (55). The lack of supralinearity in the predicted formamidinium *I-V* at 0.1 M can be attributed to this weakness of the rate theory model. In a careful comparison between a multiion Nernst–Planck model and a rate theory model with a similar central barrier height and diffusion-limited access (see Figure 1 in reference 55), Levitt found that for a concentration five times the dissociation constant (which corresponds in our case to ~0.1 M), the Nernst–Planck relation gives a supralinear *I-V*, whereas the 3B2S model, like ours, gives a sublinear *I-V*. We therefore ascribe the major weakness of our fits to the simplification that translocation is a single activated step. Nevertheless, the equilibrium rate constants should be approximately correct.

The first-ion dissociation constant, B/A = 24 mM, was similar to 44 mM predicted from the Eadie–Hofstee plot. However, to simultaneously produce a high permeance and a high affinity, it was necessary that the second ion affinity be very low. This could result from strong ion–ion repulsion between formamidiniums in the channel.

The location of Na^+ and Tl^+ binding sites in the gramicidin channel was directly investigated using ^{13}C-NMR and was found near the carbonyls of Trp 9, 11, and 13 (47). X-ray diffraction localizes the Tl^+ binding site at 9.6 Å (48), which is 11.6% of the distance through the channel from the surface. With the 3B2S method, the ionic binding site of formamidinium was located 0% into the electric field, suggesting ideal interactions outside the mouth of the channel. Methylammonium, on the other hand, behaved more like an alkali metal cation with an apparent binding site 19% into the channel. The entry step for both cations was voltage independent, which, if taken literally, suggests that first contact with the channel occurs while the ionic charge is still external to the channel.

From curve fitting with the 3B2S model, the entry rate of the second methylammonium ion (5.6×10^7 M/s) is slightly higher than that of the first ion (4.9×10^7 M/s). The exit rate of the second ion (2.3×10^8 /s) is much higher than that of the first ion (5.7×10^6 /s). This can be explained by considering that the passage of the first ion through the channel causes peptide orientation that is slightly more favorable for second ion entry, and this is consistent with the notion that the entry step (the partial dehydration) is independent of electrostatic repulsion but that the exit rate of the second ion is higher due to ion–ion repulsion within the channel (4, 6, 56). The view could be applied to ions that have the relatively much lower binding affinities such as methylammonium but not formamidinium.

Channel lifetimes

The gramicidin single channel lifetime is similar in methylammonium solution to that observed with alkali

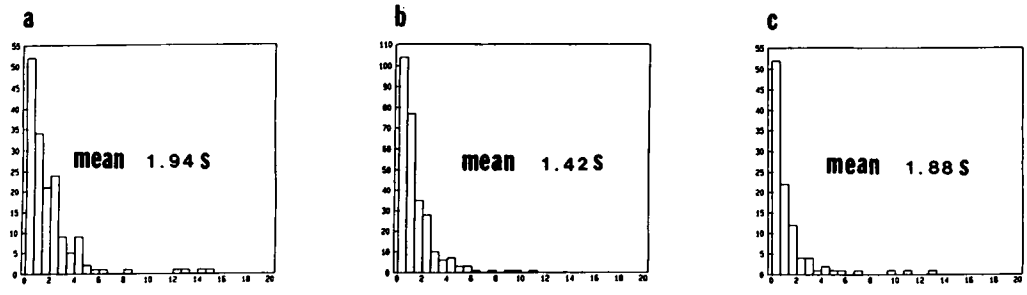

FIGURE 8 (*a–c*) The comparison of the magnitude of the stabilizing effect on the dimerization of the gramicidin A channel. All the salt solutions were 0.01 M salt + 9 mM $MgCl_2$ (*a*, formamidinium; *b*, methylammonium; *c*, hydrazinium), the applied voltage was 100 mV, and the surrounding temperature was 22.5°C (in GMO/hexadecane). All the data were collected within 1.5 h of the solution preparation.

metal cations, whereas formamidinium has markedly different effects. In formamidinium solution, the lifetime is dramatically prolonged and gets shorter (rather than longer) at higher membrane potentials. In addition, the temperature dependence and concentration dependence are significantly steeper at lower membrane potentials. The first of these effects is reminiscent of those produced by Tl^+ (25) and Ag^+ (26), which both increase channel lifetimes. The alkali metal cations also enhance channel lifetime but not as much, suggesting that formamidinium differs in occupancy and/or efficacy. It is not possible from these data to determine which, although total channel occupancy is predicted to be quite concentration independent by the 3B2S model.

The possible sites of action for this dimer stabilization effect by formamidinium can be divided into extra- and intrachannel. An extrachannel mechanism would be unlikely to be as strongly voltage dependent as we have observed. For instance, formamidinium might specifically reduce the surface tension that would then increase the channel lifetime. But, membrane potential should have little effect on this process, particularly when both interfaces are considered. To further rule out an extrachannel mechanism, we measured the channel lifetimes in 0.1 M formamidinium solution before and after addition of 1.0 M KCl. The rationale was that K^+ would compete with formamidinium for occupancy at a specific intrachannel binding site but probably not at the nonspecific lipid–water interface. Indeed, the lifetimes were significantly reduced by the addition of KCl.

This leaves intrachannel sites. It seems most likely that formamidinium would modify the lifetime by gently perturbing the channel structure. The two portions of the channel where perturbations would be expected to have large effects on the channel lifetime are the center of the dimer where six hydrogen bonds maintain the aggregated state and where methylation of the NH_2-terminal blocker dramatically decreases channel lifetime (57), and near the COOH-terminal Trp's (particularly Trp^{11}), mutations of which can dramatically affect channel lifetime (27). Distinction between these two possibilities will be considered in future publications. The indole groups of Trp side chains could influence channel function by two distinct mechanisms: by altering channel duration through direct interactions with adjacent lipid head groups and by altering the permeant ions' energy profile without contacting the ions directly (27). Perhaps additional H-bond formation or deformation between one or two Trp's and an adjacent lipid head group is possible when reorientation of a Trp near the binding site is induced by ionic occupancy. This hypothesis is consistent with the fact that Tl^+ and Ag^+ (which also bind strongly to the channel) also stabilize channel lifetimes.

On the other hand, formamidinium may affect the dimeric junction, perhaps by binding near the NH_2 termini that are expected to be somewhat flexible. The average occupancy of such a site could be very voltage dependent. However, it seems more likely that formamidinium would disrupt intermonomer hydrogen bonds by competition (58), rather than stabilize them, while bound at such a site. To exclude this hypothesis, it may be valuable to test the stabilization effect of formamidinium on the single channel lifetime in NH_2-terminal modified gramicidin A channels.

The excess single channel noise with formamidinium could be due to partial dimer ruptures, to a high frequency of slow formamidinium passages, or to formamidinium-induced changes in the channel conformation, the Trp side chain conformations, for instance. If formamidinium enhanced dimer ruptures, it should destabilize the channel, but instead it stabilizes. Furthermore, the noise would be expected to increase with voltage (since the lifetime decreases with voltage), but it does the opposite. If formamidinium slow passages were sufficiently slow and frequent to cause observable noise, the single channel conductance should be markedly impaired, but it is found to be similar to the most conductive cations. We therefore suppose that the excess noise is due to formamidinium-induced fluctuations of the gramicidin conformation that modulate channel conductance at a high frequency.

In summary, methylammonium behaves much like ammonium, whereas formamidinium is unusual among permeant cations in that it has a high binding affinity and yet a high permeability and profoundly stabilizes the dimeric channel. With the expectation that the trends in the dimer stabilization effect would be very different in *N*-acetyl gramicidin channels if the mechanism of stabilization involves the dimer junction, we have performed experiments with homo- and heterodimers using this analogue. The results of these studies will be published separately.

We thank Dr. Levitt for helpful discussions concerning modeling of the data.

This work was supported by National Institutes of Health grant GM-33361.

Received for publication 27 July 1992 and in final form 30 November 1992.

REFERENCES

1. Urry, D. W., 1971. The gramicidin A transmembrane channel: a proposed π(L,D) helix. *Proc. Natl. Acad. Sci. USA.* 68:672–676.
2. Busath, D., G. Hemsley, T. Bridal, M. Pear, K. Gaffney, and M. Karplus. 1988. Guanidinium as a probe of the gramicidin channel interior. *In* Transport Through Membranes: Carriers, Channels and Pumps. A. Pullman, J. Jortner, and B. Pullman, editors. Kluwer Academic Publishers, Dordrecht/Boston/London. 187–201.
3. Hladky, S. B., and D. A. Haydon. 1972. Ion transfer across lipid membranes in the presence of gramicidin A. I. Studies of the

unit conductance channel. *Biochim. Biophys. Acta.* 274:294–312.

4. Urban, B. W., S. B. Hladky, and D. A. Haydon. 1980. Ion movements in gramicidin pores. An example of single-file transport. *Biochim. Biophys. Acta.* 602:331–354.
5. Hladky, S. B., and D. A. Haydon. 1984. Ion movements in gramicidin channels. *Curr Top Membr Transp* 21:327–372.
6. Finkelstein, A., and O. S. Andersen. 1981. The gramicidin A channel: a review of its permeability characteristics with special reference to the single-file aspect of transport. *J. Membr. Biol.* 59:155–171.
7. Eisenman, G., J. Sandblom, and J. Hagglund. 1983. Electrical behavior of single-filing channels. *In* Structure and Function in Excitable Cells. W. Chang, I. Tasaki, W. Adelman, and R. Leuchtag, editors. Plenum Publishing Corporation, New York. 383–413.
8. Andersen, O. S. 1984. Gramicidin channels. *Annu. Rev. Physiol.* 46:531–548.
9. Hille, B. 1971. The permeability of the sodium channel to organic cations in myelinated nerve. *J. Gen. Physiol.* 58:599–619.
10. Hille, B. 1973. Potassium channels in myelinated nerve. *J. Gen. Physiol.* 61:669–686.
11. Dwyer, T. M., D. J. Adams, and B. Hille. 1980. The permeability of the endplate channel to organic cations in frog muscle. *J. Gen. Physiol.* 75:469–492.
12. Eisenman, G., S. Krasne, and S. Ciani. 1975. The kinetic and equilibrium components of selective permeability mediated by nactin- and valinomycin-type carriers having systematically varied degrees of methylation. *Ann. NY Acad. Sci.* 264:34–60.
13. Eisenman, G., S. Krasne, and S. Ciani. 1976. Further studies on ion selectivity. *In* Ion and Enzyme Electrodes in Medicine and in Biology. M. Kessler, L. Clark, D. Lubbers, I. Silver, and W. Simon. editors. Urban and Schwarzenberg, Munich/Berlin/Vienna. 3–22.
14. Hemsley, G., and D. Busath. 1991. Small iminium ions block gramicidin channels in lipid bilayers. *Biophys. J.* 59:901–907.
15. Turano, B., M. Pear, and D. Busath. 1992. Gramicidin channel selectivity. Molecular mechanics calculations for formamidinium, guanidinium, and acetamidinium. *Biophys. J.* 63:152–161.
16. Rudnev, V. S., L. N. Ermishkin, L. A. Fonina, and YuG Rovin. 1981. The dependence of the conductance and lifetime of gramicidin channels on the thickness and tension of lipid bilayers. *Biochim. Biophys. Acta.* 642:196–202.
17. Elliot, J. R., D. Needham, J. P. Dilger, and D. A. Haydon. 1983. The effects of bilayer thickness and tension on gramicidin single-channel lifetime. *Biochim. Biophys. Acta.* 735:95–103.
18. Kolb, H. A., and E. Bamberg. 1977. Influence of membrane thickness and ion concentration on the properties of the gramicidin A channel. Autocorrelation, spectral power density, relaxation and single-channel studies. *Biochim. Biophys. Acta.* 464:127–141.
19. Huang, H. W. 1986. Deformation free energy of bilayer membrane and its effect on gramicidin channel lifetime. *Biophys. J.* 50:1061–1070.
20. Helfrich, P., and E. Jakobsson. 1990. Calculation of deformation energies and conformations in lipid membranes containing gramicidin channels. *Biophys. J.* 57:1075–1084.
21. Ring, A. 1992. Influence of ion occupancy and membrane deformation on gramicidin A channel stability in lipid membranes. *Biophys. J.* 61:1306–1315.
22. Ring, A., and J. Sandblom. 1983. Measurement of channel lifetime in artificial lipid membranes: dimerization kinetics of gramicidin A. *J. Membr. Sci.* 16:319–337.
23. Bamberg, E., and P. Lauger. 1974. Temperature-dependent properties of gramicidin A channels. *Biochim. Biophys. Acta.* 367:351–375.
24. Urry, D. W., S. Alonso-Romanowski, C. M. Venkatachalam, R. J. Bradley, and R. D. Harris. 1984. Temperature dependence of single channel currents and the peptide libration mechanism for ion transport through the gramicidin A transmembrane channel. *J. Membr. Biol.* 81:205–217.
25. Andersen, O. S., and J. Procopio. 1979. Ion entry into gramicidin A channels is diffusion-limited. *Bull. NY Acad. Med.* 55:403.
26. McBride, D. W. 1981. Anomalous mole fraction behavior, momentary block, and lifetimes of gramicidin A in silver and potassium fluoride solutions. Ph.D. thesis. University of California, Los Angeles.
27. Becker, M. D., D. V. Greathouse, R. E. Koeppe, II, and O. S. Andersen. 1991. Amino acid sequence modulation of gramicidin channel function: effects of tryptophan-to-phenylalanine substitutions on the single-channel conductance and duration. *Biochemistry.* 30:8830–8839.
28. Eyring, H., R. Lumry, and J. W. Woodbury. 1949. Some applications of modern rate theory to physiological systems. *Rec. Chem. Prog.* 10:100–114.
29. Hille, B. 1991. Ionic Channels of Excitable Membranes. 2nd ed. Sinauer Associates Inc., Sunderland, MA. 607 pp.
30. Busath, D., and G. Szabo. 1988. Low conductance gramicidin A channels are head-to-head dimers of $\beta^{6.3}$-helices. *Biophys. J.* 53:689–695.
31. Busath, D., and G. Szabo. 1981. Gramicidin forms multi-state rectifying channels. *Nature (Lond.).* 294:371–373.
32. Neher, E., J. Sandblom, and G. Eisenman. 1978. Ionic selectivity, saturation, and block in gramicidin A channels. II. Saturation behavior of single channel conductances and evidence for the existence of multiple binding sites in the channel. *J. Membr. Biol.* 40:97–116.
33. Apell, H. J., E. Bamberg, and P. Lauger. 1979. Effects of surface charge on the conductance of the gramicidin channel. *Biochim. Biophys. Acta.* 552:369–378.
34. Andersen, O. S. 1983. Ion movement through gramicidin A channels. Interfacial polarization effects on single-channel current measurements. *Biophys. J.* 41:135–146.
35. Begenisich, T. B., and M. D. Cahalan. 1980. Sodium channel permeation in squid axons. I. Reversal potential measurements. *J. Physiol. (Lond.).* 307:217–242.
36. Eisenman, G., J. Sandblom, and E. Neher. 1977. Ionic selectivity, saturation, binding, and block in the gramicidin A channel: a preliminary report. *In* Metal-Ligand Interactions in Organic Chemistry and Biochemistry. Vol. 9. Part 2. B. Pullman and N. Goldblum, editors. Reidel Publishing Company, Dordrecht-Holland. 1–36.
37. Levitt, D. G. 1986. Interpretation of biological ion channel flux data-reaction-rate versus continuum theory. *Annu. Rev. Biophys. Biophys. Chem.* 15:29–57.
38. Jakobsson, E., and S. W. Chiu. 1987. Stochastic theory of ion movement in channels with single-ion occupancy. Application to sodium permeation of gramicidin channels. *Biophys. J.* 52:33–45.
39. Busath, D., and G. Szabo. 1988. Permeation characteristics of gramicidin conformers. *Biophys. J.* 53:697–707.
40. Levitt, D. G. 1978. Electrostatic calculations for an ion channel. II. Kinetic behavior of the gramicidin A channel. *Biophys. J.* 22:221–248.
41. Eisenman, G., J. Sandblom, and E. Neher. 1978. Interaction in cation permeation through the gramicidin channel. Cs, Rb, K, Na, Li, Tl, H, and effects of anion binding. *Biophys. J.* 22:307–340.

42. Eisenman, G., and R. Horn. 1983. Ionic selectivity revisited: the role of kinetic and equilibrium processes in ion permeation through channels. *J. Membr. Biol.* 76:197–225.

43. Urban, B. W., S. B. Hladky, and D. A. Haydon. 1978. The kinetics of ion movements in the gramicidin channel. *Fed. Proc.* 37:2628–2632.

44. Hladky, S. B., B. W. Urban, and D. A. Haydon. 1979. Ion movements in the gramicidin pore. *In* Membrane Transport Processes. C. F. Stevens and R. W. Tsien, editors. Raven Press, New York. 89–103.

45. Decker, E. R., and D. G. Levitt. 1983. Comparison of the gramicidin A potassium/sodium permeability and single channel conductance ratio. *Biochim. Biophys. Acta.* 730:178–180.

46. Myers, V. B., and D. A. Haydon. 1972. Ion transfer across lipid membranes in the presence of gramicidin A. II. The ion selectivity. *Biochim. Biophys. Acta.* 274:313–322.

47. Urry, D. W., K. U. Prasad, and T. L. Trapane. 1982. Location of monovalent cation binding sites in the gramicidin channel. *Proc. Natl. Acad. Sci. USA.* 79:390–394.

48. Olah, G. A., H. W. Huang, W. H. Liu, and Y. L. Wu. 1991. Location of ion-binding sites in the gramicidin channel by x-ray diffraction. *J. Mol. Biol.* 218:847–858.

49. Heckmann, K. 1965. Zur theorie der "single file" - diffusion, II. *Z. Phys. Chem.* 46:1–25.

50. Hladky, S. B. 1972. The mechanism of ion conduction in thin lipid membranes containing gramicidin A. Ph.D. thesis. Cambridge University, Cambridge, UK.

51. Hille, B., and W. Schwarz. 1978. Potassium channels as multi-ion single-file pores. *J. Gen. Physiol.* 72:409–442.

52. Hinton, J. F., J. Q. Fernandez, D. C. Shungu, W. L. Whaley, R. E. Koeppe, and F. S. Millett. 1988. Tl-205 nuclear magnetic resonance determination of the thermodynamic parameters for the binding of monovalent cations to gramicidin A and C. *Biophys. J.* 54:527–533.

53. Urry, D. W., T. L. Trapane, C. M. Venkatachalam, and K. U. Prasad. 1985. Carbon-13 nuclear magnetic resonance study of potassium and thallium ion binding to the gramicidin A transmembrane channel. *Can. J. Chem.* 63:1976–1981.

54. Hinton, J. F., R. E. Koeppe, F. S. Millett, J. A. Paczkowski, D. Shungu, and W. L. Whaley. 1986. Equilibrium binding constants for Tl^+ with gramicidin-A, gramicidin-B, and gramicidin-C in a lysophosphatidylcholine environment determined by Tl-205 nuclear magnetic-resonance spectroscopy. *Biophys. J.* 49:571–577.

55. Levitt, D. G. 1982. Comparison of Nernst-Planck and reaction-rate models for multiply occupied channels. *Biophys. J.* 37:575–587.

56. Sandblom, J., G. Eisenman, and J. Hagglund. 1983. Multioccupancy models for single filing ionic channels: theoretical behavior of a four-site channel with three barriers separating the sites. *J. Membr. Biol.* 71:61–78.

57. Szabo, G., and D. W. Urry. 1979. N-acetyl gramicidin: single-channel properties and implications for channel structure. *Science (Wash. DC).* 203:55–57.

58. Urry, D. W., A. Spisni, M. A. Khaled, M. M. Long, and L. Masotti. 1979. Transmembrane channels and their characterization in phospholipid structures. *Int. J. Quantum. Chem. Quantum. Biol. Symp.* 6:289–303.